Available online at www.sciencedirect.com

ScienceDirect

Procedia Engineering 139 (2016) 123 – 133

Procedia Engineering

www.elsevier.com/locate/procedia

MRS Singapore – ICMAT Symposia Proceedings

8th International Conference on Materials for Advanced Technologies

Synchrotron X-ray Micro-diffraction – Probing Stress State in Encapsulated Thin Silicon Solar Cells

Sasi Kumar TIPPABHOTLA[1#], Ihor RADCHENKO[1], Karthic Narayanan RENGARAJAN[1], Gregoria ILLYA[2], Vincent HANDARA[2], Martin KUNZ[3], Nobumichi TAMURA[3], Arief Suriadi BUDIMAN[1]

[1]SUTD Singapore University of Technology and Design, Singapore, [2]Center for Solar Photovoltaics (CPV), Surya University, Indonesia,
[3]Advanced Light Source (BL 12.3.2), LBNL, Berkeley, CA, USA,
[#]Corresponding author, sasi_kumar@mymail.sutd.edu.sg,

Abstract

There has been a strong commercial push towards thinner silicon in the solar photovoltaic (PV) technologies due to the significant cost reduction associated with it. However, in current products made from crystalline solar cell technologies, normal in-plane tensile stress resulting in fracture of silicon cells are observed. To further understand this phenomenon, the synchrotron X-ray micro-diffraction tool was used to perform stress measurements and mapping of the solar cells in the vicinity of the most typically observed crack initiation location, the solder joint. This technique is unique as it has the capabilities to quantitatively determine the stresses and map these stresses with a micron resolution, all while the silicon cells are in encapsulation. A fundamental understanding of the stress magnitudes as well as microstructural characteristics that could lead to crack initiation and propagation could be obtained with this technique. This also confirms that the control of mechanical stress is the key to enable thin silicon solar cell technologies in the coming years.

Selection and/or peer-review under responsibility of the scientific committee of Symposium 2015 ICMAT

Keywords:

1. Introduction

Crystalline silicon solar photovoltaic modules are sandwich structures consisting of materials with different

Selection and/or peer-review under responsibility of the scientific committee of Symposium 2015 ICMAT
doi:10.1016/j.proeng.2015.09.241

coefficients of thermal expansion (CTE) and thicknesses as shown in Figures 1a and 1b. They tend to develop internal residual stresses due to differential thermal strain in constituent materials due to CTE mismatch during module making process involving high temperature and pressure. The internal residual stresses are detrimental to the reliability of the solar cells and modules as they act as stress localization centres and initiate cracking and failure during the operation of the module [1- 8] as shown in Figures 1c to 1f. Further with the thinning of the silicon wafer to improve cell efficiency and reduce cost of the silicon solar cell modules, the silicon cell becomes even more susceptible to the residual stress and cracking [3]. In this scenario, evaluation of the residual stress in the silicon solar cells is of prime importance to improve the design life and reliability of the solar cell modules.

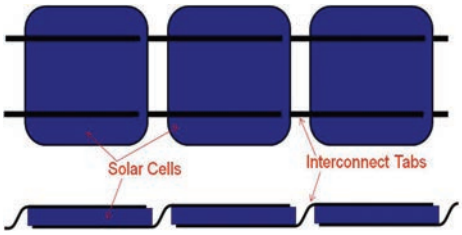

(a)

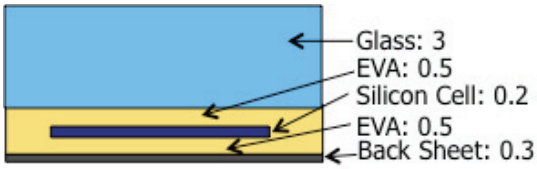

(b) Module components with thickness in mm

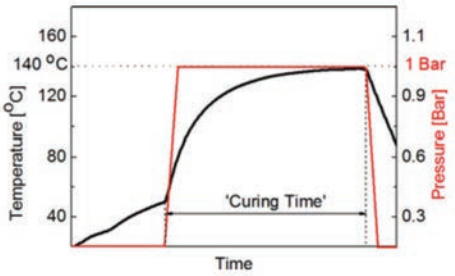

(c)

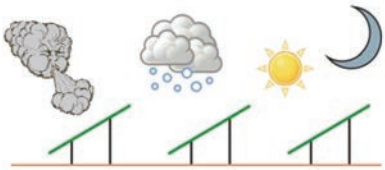

(d)

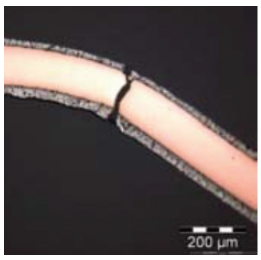

(e)

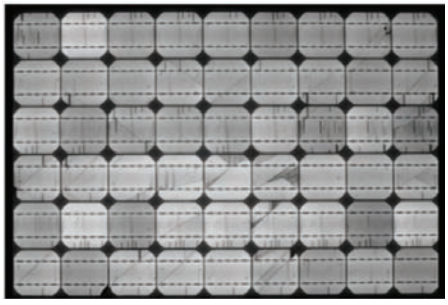

(f)

Fig. 1: (a) Solar Cell Strings, (b) Schematic of a solar cell module showing layer thickness in mm, (c) Temperature and pressure variation in module lamination process [6], (d) Loads on solar modules in operation [7], (e) Cracked solar cell interconnect ribbon [7], (f) Electroluminescence image of solar panel showing cracks in cells [8]

Researchers used different experimental and numerical simulations to evaluate the residual stress and also stress due to operational loads [9-15]. Particularly Sander et al. [4,5] used mechanical loading experiments to characterize the stress and cracks by electroluminescence (EL). Dietrich et al. [7] and Pander et al. [8] used both finite element simulations and EL testing to characterize stress and fracture of solar cell modules. Dietrich et al. [9] and Osama Hassan et al. [10] used finite element analysis to characterize stress in solar modules and interconnect. Vidya Ganapathi et al. [11] used infrared birefringence imaging to evaluate residual stress in multi-crystalline silicon. Fang Li [2] studied the stress in the silicon wafers using digital photo-elasticity. G. Saru et al. [13] used Raman spectroscopy to evaluate residual stress in the silicon solar cells near solder joint. A.S. Budiman et al. [14, 15] used Synchrotron X-ray Micro-diffraction to evaluate silicon stress in the encapsulated solar cell modules made of mono-crystalline silicon cells with back metallization. While the finite element simulations are limited by the capability of the material models used, most of the experimental methods are limited to the surface level stress measurements as they can not penetrate the encapsulated solar cell module to probe the stress in the silicon cell. Out of all the techniques listed above, Synchrotron X-ray Micro-Diffraction (μSXRD) is shown to be capable of penetrating the encapsulated solar cell module to evaluate the residual stress in the crystalline silicon solar cell [14, 15]. This report is aimed to explain the experimental setup and procedure of evaluating residual stress in the silicon of solar cell module. This report also touches upon the sample requirements, limitations on the sample size and challenges associated with the method and some interesting future prospects using this technique such as in-situ and in-operando experiments on the solar cell modules.

2. Synchrotron X-ray Micro-Diffraction – Experimental Setup and Procedure

Synchrotron is a particle accelerator with a circumference of about 1 km approximately. It converts the energy of the fast moving electrons into very high-energy polychromatic X-ray beam [16]. There are synchrotron facilities in several national and international laboratories of USA, Europe, India, Singapore, etc. [16]. Each synchrotron sources several X-ray beams suitable for different purposes, which are called beamlines. Our micro-diffraction experiments were conducted at Beamline 12.3.2 of the Advanced Light Source (ALS), Lawrence Berkeley National Laboratory (LBNL), Berkeley, California [17]. A typical setup of ALS beamline 13.3.2 was shown in Figure 2.

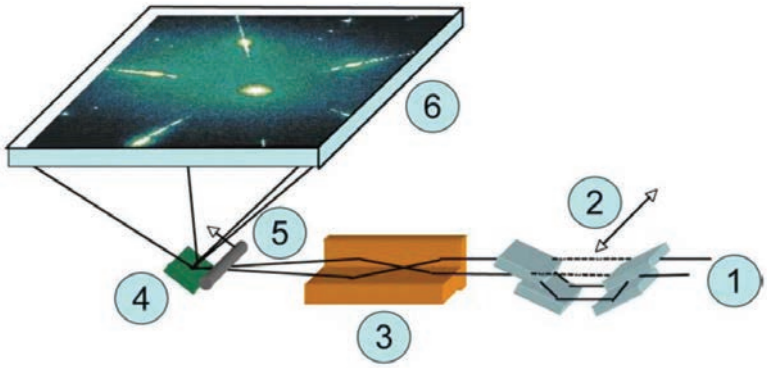

Fig. 2: Schematic layout of the beamline 12.3.2 A has six key elements: (1) a brilliant polychromatic x-ray source; (2) a non-dispersive monochromator that can be moved into or out of the beam; (3) achromatic focusing optics; (4) a precision sample stage; (5) an x-ray absorbing wire; and (6) an x-ray sensitive area detector (Courtesy of Ice & Pang [19])

In the beamline, the polychromatic X-Ray beam produced from a superconductor magnet source of synchrotron is

refocused at the entrance of the experimental hutch by a platinum-coated silicon toroidal mirror, operating at a grazing angle of 4.5mrad. Final focusing is done by Kirkpatrick-Baez mirrors consisting of an orthogonal pair of 100 mm-long tungsten-coated silicon substrate bent to an elliptical shape. Unlike the normal laboratory X-ray, the X-ray beam coming out of this beamline is of high intensity and highly collimated. Further this is a high energy (5 - 20 keV), polychromatic beam of 0.8 microns diameter and hence it can penetrate the samples that are normally impossible for a laboratory X-ray to pass through. In case of encapsulated solar cell module, the synchrotron X-ray can penetrate the sample to probe the stress in the silicon cell. A detailed description of the synchrotron and the beamline construction are beyond the scope of this report and are readily available in references [16-20].

The experimental sample we used here is a 175x175 mm mini module consisting of a single 125x125 mm mono-crystalline back contact solar cell as shown in Figure 3a. The region that was actually scanned by X-rays is zoomed out in Figure 3a. Further we used a transparent back sheet instead of a regular back sheet in order to make it transparent to x-ray beam. The front glass is an industry standard tempered glass and the encapsulant is EVA, which is also an industry standard. Figure 3b shows schematic micro diffraction setup of the mini solar module and Figure 3c shows picture of the actual setup.

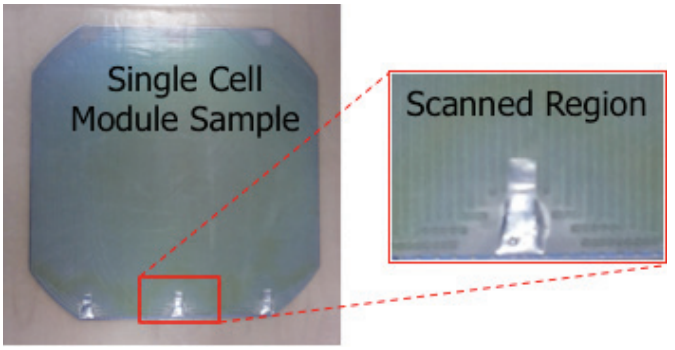

(a)

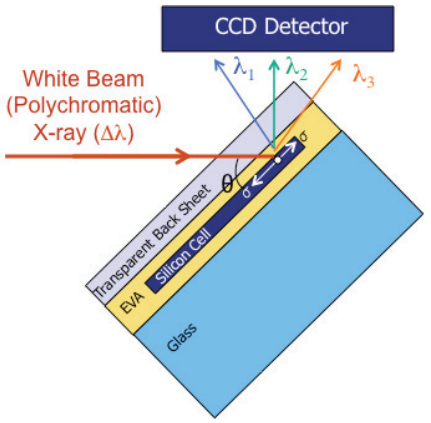

(b)

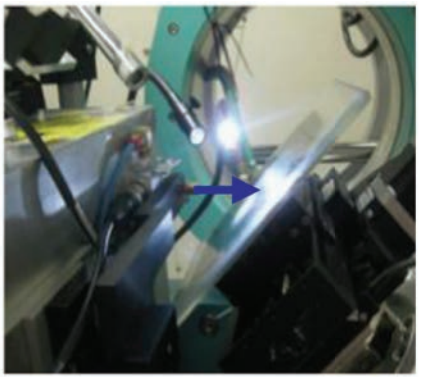

(c)

Fig.3: (a) Mini solar module used for testing, (b) Schematic of Test Setup, (c) Actual picture of the Test Setup

The sample was mounted on the stage as shown in Figures 3b and 3c with its back (metallization side of the solar cell) facing the X-ray beam. The sample stage that is capable of moving in X, Y and Z directions was adjusted to focus the X-ray beam on the sample as required by the experiment.

The sample stage is capable of automatic raster scanning [20] and once sample is setup with optimal focus, the automatic raster scan can be invoked. The system conducts a pixel-by-pixel scan of the selected region of the sample (Figure 4) and generates diffraction pattern for each pixel. The spacing between pixels can be selected to get reasonable approximation to continuity. We selected 0.1 mm as the spacing and exposed each spot for 1.5 sec to get reasonable brightness of the diffraction pattern. The typical Laue diffraction pattern for silicon is shown in Figure 4. Once the scan is complete it generates as many diffraction patterns as the number of pixels. One of these diffraction patterns should be indexed manually using XMAS software [20] to identify the miller indices of the planes that produced the diffraction spots in the pattern as shown in Figure 4. Later this indexed pattern can be used to index the all the remaining diffraction patterns automatically by XMAS [20]. Once all the patterns are indexed, the characteristics, local curvature and strain at the spots can be calculated by comparing the crystal lattice parameters obtained from this scan with the baseline silicon crystal lattice parameters following Braggs law and Laue condition [20] as explained in the following section.

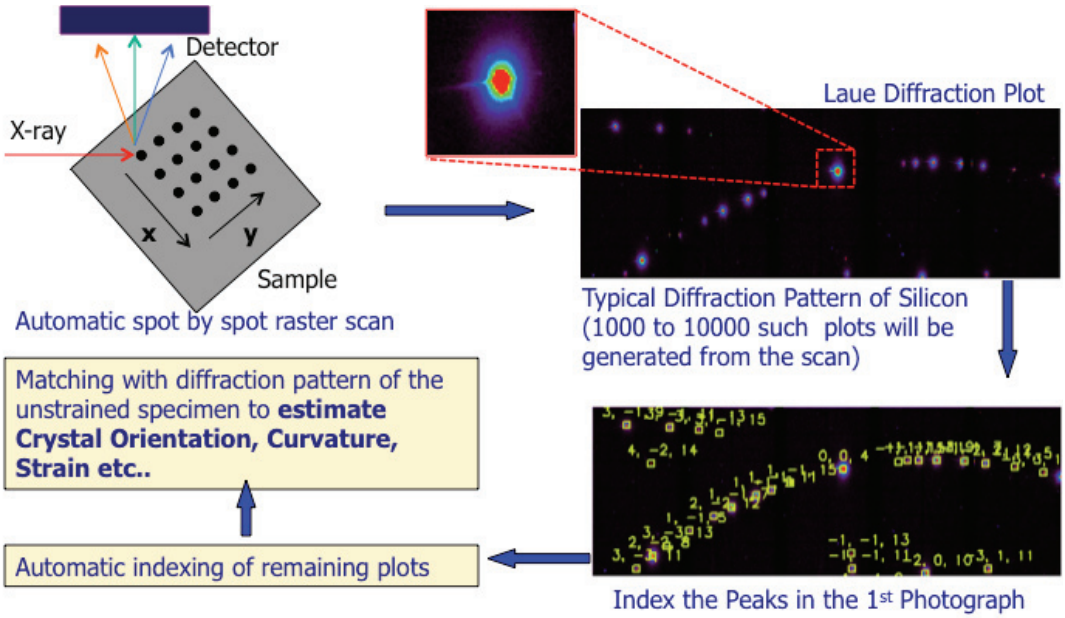

Fig. 4: Typical Process Map of Automated µSXRD at ALS BL-12.3.2 and Subsequent Analysis using XMAS

3. Results & Discussion

3.1 Residual Stress Evaluation from White Beam Laue Diffraction Images

Though Bragg's law is the underlying principle for the X-ray diffraction, the specific case of single crystal sample subjected to white beam X-ray follows Laue diffraction condition, named after Von Laue. The resulting diffraction pattern is commonly known as Laue diagram (Figure 4) and each spot in it is called as Laue spot. Each Laue spot is generated by a specific X-ray energy selected by the given lattice plane. A specialized software

program, XMAS [20] can then be used to analyze these patterns and index them as shown in Figure 4, identifying individual patterns from each grain. From this analysis it is possible to determine the orientation matrix of each grain. As our sample is single crystal silicon cell, each grain has same orientation. Further the deviatoric strain can be derived from the Laue diffraction pattern based on the homogeneity property, which states that the coordinates of a given point inside the un-deformed unit cell remain unaffected in the deformed cell as shown in the equation 1 below [20].

$$\boldsymbol{R_0 X_0 = R X} \tag{1}$$

Where X_0 and X are the coordinate positions of a point, expressed in the Cartesian coordinate system attached to the unit cell in the undeformed and deformed unit cells respectively and R_0 and R are the transformation matrices converting Cartesian coordinates into unit cell coordinates for the undeformed and deformed unit cell respectively. Equation 1 can be rewritten as shown below to define the deformation matrix, T mapping the undeformed state to the deformed state.

$$\boldsymbol{X = R^{-1} R_0 X_0 = T X_0} \tag{2}$$

Now the deviatoric strain can be computed by the equation 3 given below.

$$\boldsymbol{\epsilon'_{ij} = \frac{1}{2}\left(T_{ij} + T_{ji}\right) - \delta_{ij}} \tag{3}$$

Where 'δ_{ij}' is the Dirac-delta function. The deviatoric stress is then found using Hooke's law (Equation 4).

$$\boldsymbol{\sigma'_{ij} = C_{ijkl} \epsilon'_{kl}} \tag{4}$$

Further references [18-20] discuss the stress derivation more elaborately. Figures 5a-10a show maps of different components of the deviatoric stress in our silicon solar cell sample (Figure 3a) calculated directly using XMAS from the Laue diffraction plots. Figures 5b-10b show histograms of the respective stress map in order to highlight the confidence level of a max stress value on the stress map. It can be seen that the deviatoric stress values in the directions of xx, yy and zz are not very significant. This could be because much of the stresses in these directions belong to the hydrostatic stress, which is not captured by the Laue technique. The other deviatoric stresses, which are the shear stresses - $\boldsymbol{\sigma'_{xy}}$, $\boldsymbol{\sigma'_{xz}}$ and $\boldsymbol{\sigma'_{yz}}$ are quite high (max values exceeding 500 MPa) indicating potential device or performance-related issues due to high distortional stress in the silicon surrounding the solder joint. However, it is evident from the stress maps that the shear stresses are mostly following the metallization lines on the silicon solar cell, and not necessarily due to the solder joint itself. The large values of the shear stresses $\boldsymbol{\sigma'_{xz}}$ and $\boldsymbol{\sigma'_{yz}}$ are expected considering the asymmetric bending of the silicon cell, which induces shear stresses in XZ and YZ planes. Interestingly $\boldsymbol{\sigma'_{xy}}$ is also quite significant given the biaxial stress state with the normal stress in one direction is larger than the other due to the metallization lines that are mostly going in one direction. In the context of silicon cell bending and high stress concentration near the solder joint, the shear stresses are probably not a big concern for the silicon material integrity, compared to the large values of the normal stresses. Especially if the normal stresses are tensile as they could lead to cracking and fracture of the solar cells. This problem will be further aggravated if there are micro cracks / defects (carried forward from the wafer cutting process) in the silicon cell. So accurate estimation of the normal stresses in the solar cell is of prime importance and the deviatoric stress mapping performed in this section is not able to provide complete information of the normal stresses. In order to get total normal stresses in each direction, energy scan of the sample at each pixel is required which is rather time consuming and may not be very accurate. Next section explains the process, which was used to estimate the bending stress (which is the most significant component of the normal stress) in the silicon cell through an indirect approach using a modified Stoney's equation.

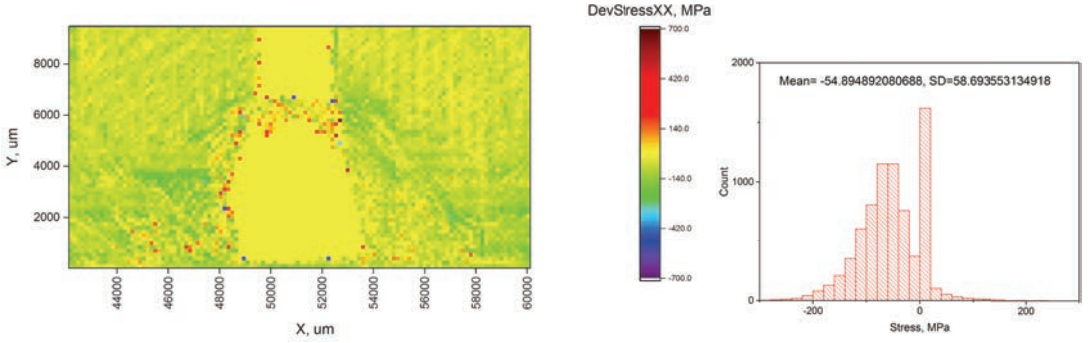

(a) Stress Map (b) Histogram

Fig. 5: Silicon Cell Deviatoric Stress Component in X-direction, σ'_{xx} (MPa) from XMAS

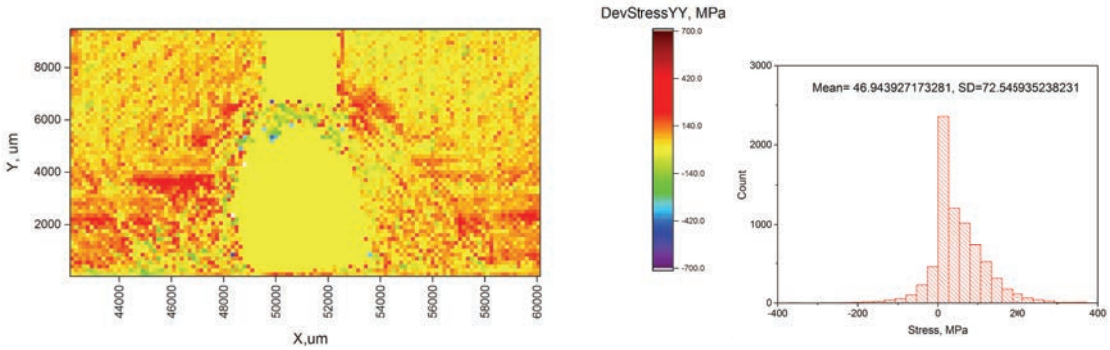

(a) Stress Map (b) Histogram

Fig. 6: Silicon Cell Deviatoric Stress Component in Y-direction, σ'_{yy} (MPa) from XMAS

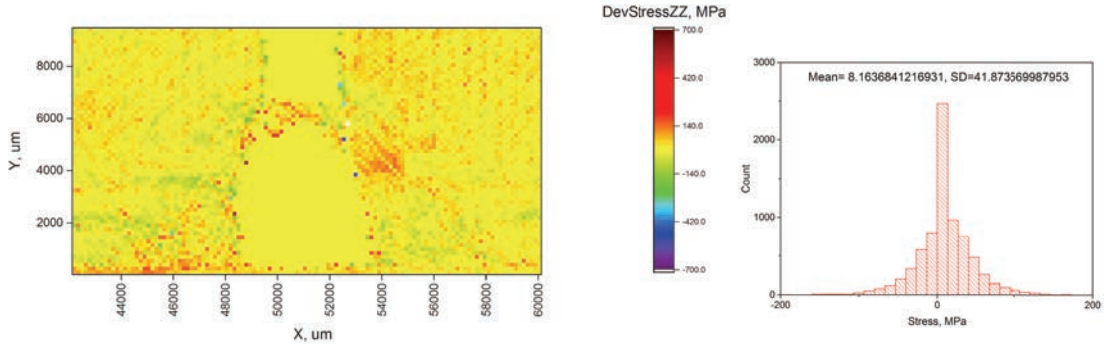

(a) Stress Map (b) Histogram

Fig. 7: Silicon Cell Deviatoric Stress Component in Z-direction, σ'_{zz} (MPa) from XMAS

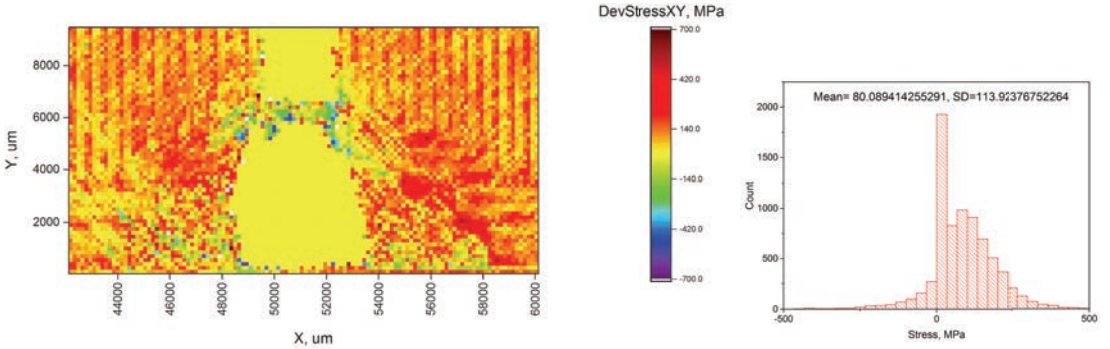

(a) Stress Map (b) Histogram

Fig. 8: Silicon Cell Deviatoric Stress Component in XY-Plane, σ'_{xy} (MPa) from XMAS

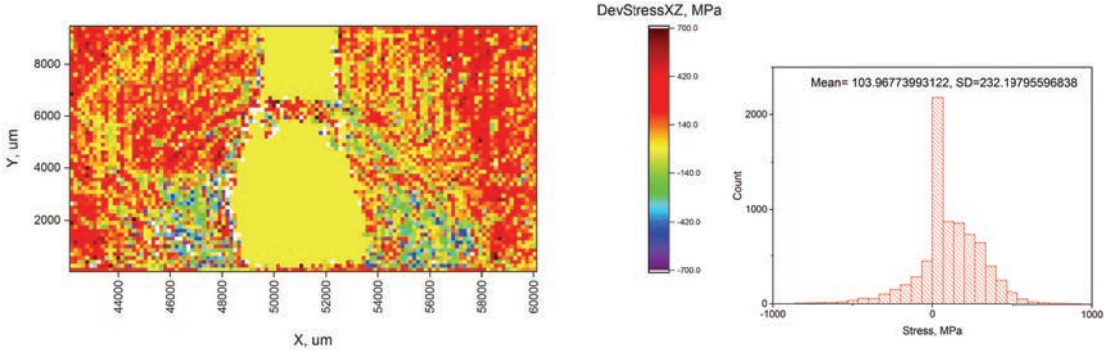

(a) Stress Map (b) Histogram

Fig. 9: Silicon Cell Deviatoric Stress Component in XZ-Plane, σ'_{xz} (MPa) from XMAS

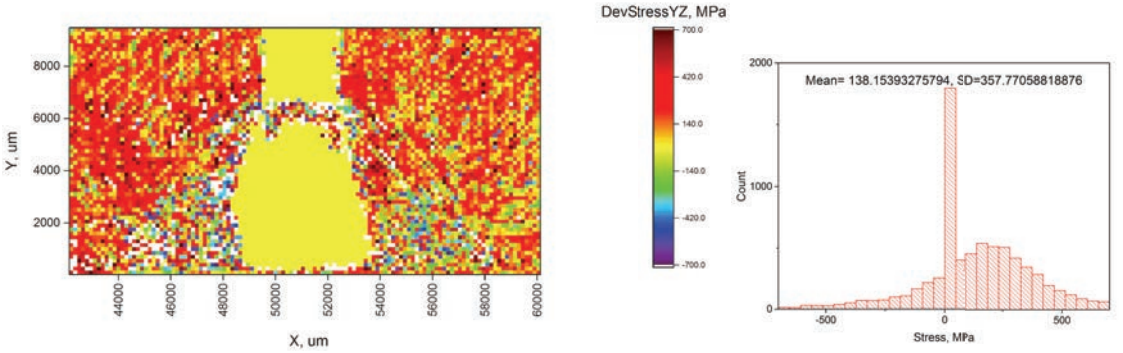

(a) Stress Map (b) Histogram

Fig. 10: Silicon Cell Deviatoric Stress Component in YZ-Plane, σ'_{yz} (MPa) from XMAS

3.2 Residual Stress Evaluation Using Stoney's Equation

To circumvent the problem discussed in the previous section, we adapted to an indirect method of stress calculation using the relative change in orientation of unit cell (θ) as a measure of curvature and then Stoney's equation, as outlined in K. Chen et al. [21-22]. This is because unlike the stress (or strain), the relative change in the unit cell orientation will be negligibly affected by the penetration of the X-ray across the sample due to the uniformity of the diffraction volume across the scan. Hence any error resulting from the distortion of the diffraction signal will remain constant over the scan and cancel out during calculation relative orientation change of the unit cell (θ). Now curvature of the unit cell about any direction can be calculated by differentiating the respective θ with the respective spacial coordinate, for example curvature about Y-axis (in XZ plane) can be calculated as shown below in equation 5.

$$\boldsymbol{\kappa_y} = \frac{\boldsymbol{d\theta_{xz}}}{\boldsymbol{dx}} \tag{5}$$

Similarly curvatures from all the three directions (X, Y and Z) can be obtained. Using Stoney's equation one can calculate the stress in the thin film when the curvature is known [21-22] as shown in equation 6 below. From the geometry of the sample near the solder joint, it can be understood that the bending stress in X-direction is significant compared to the other two components and hence we calculated the X-direction stress in silicon.

$$\boldsymbol{\sigma_{xx}} = \frac{\boldsymbol{E_s t_s^2}}{\boldsymbol{12 t_f (1-\upsilon_f)}} \boldsymbol{\kappa_y} \tag{6}$$

Where E, t and ν are Young's modulus, thickness and Poisson's ratio, respectively. And κ_y is the local crystal curvature calculated as explained above. The subscripts s and f denote the substrate (metallization) and film (silicon cell) respectively. The Stoney's equation used here is modified to suite the localized geometry of our measurement, per [21].

The silicon stress map is shown in Figure 11 below. The order of the magnitude of the stress is quite convincing for the lamination process involving high temperature difference of 125^0 C from the room temperature and also intuitively the bending stress in silicon wafer is following the bending pattern one would expect in the presence of the given solder joint. The max stress is of the order of 300 MPa and it is occurring right at the solder joint (either side, almost symmetric) and decaying with the increasing distance from the solder joint.

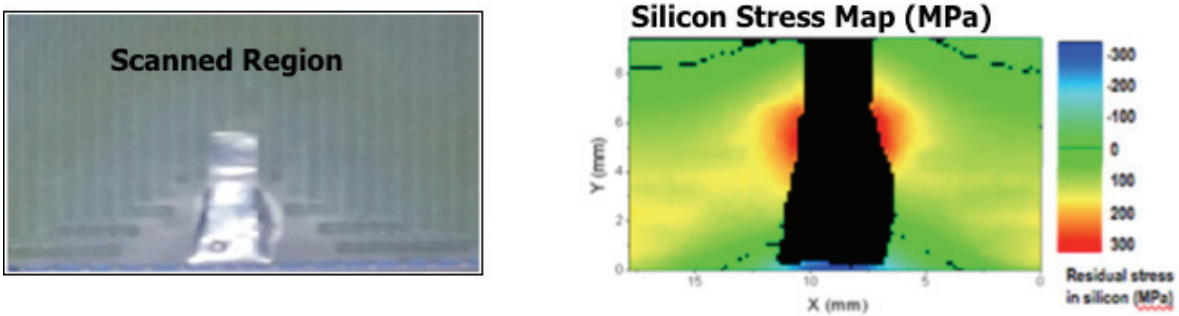

Fig. 11: Silicon Stress Map in the mini module corresponding to the scanned region

4. Conclusions

Mechanical stress and fracture are the origins of failures of the solar PV cells during their fabrication as well as their operations in the fields. Thus it is very important to have the tools to characterize them in a more quantitative manner. Through the studies in this article, μSXRD used for residual stress evaluation in encapsulated solar cell and it proved to be a very useful technique with unique capabilities to characterize stress quantitatively especially once the solar cells are laminated, this tool has proved to be perhaps the only practical technique that could provide the capability to study the stress in the silicon solar cells. In this article we also explained how and why the direct stress calculation method is not accurate for the estimation of solar cell residual stress and how Stoney's equation can be used to predict the realistic stress. Further experiments such as in-situ and in-operando evaluation of the solar cell modules can be devised using this technique to get complete understanding of the stress evolution, fracture of the solar cell modules. This method of white beam Laue diffraction can also be used to evaluate residual stress in polycrystalline silicon solar cells also but there is a limitation relating to grain size in the sample. When there are too many grains in an image, the soft- ware is unable to determine which spots correspond to which grains, and cannot analyse the image. Therefore, white x rays are used when the grain size is comparable to or larger than the beam size. Our current experiments are aimed at evaluating the residual stress in polycrystalline silicon solar cell with grain size much higher than the beam size (1 μm).

Acknowledgements

The authors would like to thank for critical discussion with Solar Energy Research Institute (Singapore), Sunpower Corporation (USA) and REC Solar (Singapore). Critical support and infrastructure provided by Singapore University of Technology and Design (SUTD) during the manuscript preparation is highly appreciated. SK and ASB also gratefully acknowledge the funding and support from National Research Foundation (NRF)/Economic Development Board (EDB) of Singapore for the project of Enabling Thin Silicon Technologies for Next Generation, Lower Cost Solar PV Systems.

References

[1] M. Gabor et al., Soldering induced damage to thin Si solar cells and detection of cracked cells in modules. 21st European Photovoltaic Solar Energy Conference, 2006.
[2] J. Wendt, M. Träger, M. Mette, A. Pfennig, B. Jaeckel, The link between mechanical stress induced by soldering and micro damages in silicon solar cells, in: Proceedings of EUPVSEC, 2009, pp. 3420–3423.
[3] W. P. Mulligan, M. A. Carandang, M. Dawson, D. M. D. Ceuster, C. N. Stone, and R. M. Swanson, 21st European Photovoltaic Solar Energy Conference and Exhibition WIP-Munich, Dresden, Germany, 2007.
[4] M. Sander, S. Dietrich, M. Pander, S. Schweizer, M. Ebert, and J. Bag- dahn. Investigations on crack development and crack growth in em- bedded solar cells. Proceedings of SPIE –The International Society for Optical Engineering, 2011.
[5] M. Sander, S. Dietrich, M. Pander, M. Ebert, and J. Bagdahn. System- atic investigation of cracks in encapsulated solar cells after mechanical loading. *Solar Energy Materials & Solar Cells*, 111:82–89, 2013.
[6] Heng-Yu Li, Yun Luo, Christophe Ballif, and Laure-Emmanuelle Perret-Aebi, Fast and Nondestructive Detection on the EVA Gel Content in Photovoltaic Modules by Optical Reflection, IEEE JOURNAL OF PHOTOVOLTAICS, VOL. 5, NO. 3, MAY 2015
[7]. S. Dietrich, M. Pander, R. Meier, S.-H. Schulze, M. Ebert, MECHANICAL ISSUES ON SOLAR MODULES AND ENCAPSULATED COMPONENTS, PVMRW 2011
[8] Pander, M. Fraunhofer, Dietrich, S., Schulze, S.-H., Eitner, U., Ebert, M., Thermo-mechanical assessment of solar cell displacement with respect to the viscoelastic behaviour of the encapsulant, IEEE 2011
[9] S. Dietrich, M. Pander, M. Sander, S.H. Schulze, and M. Ebert. Mechanical and Thermo-Mechanical Assessment of Encapsulated Solar Cells by Finite-Element-Simulation. Proceedings of SPIE –The International So- ciety for Optical Engineering, 2008.
[10] Osama Hassan et al., "Finite Element Modeling, Analysis, and Life Prediction of Photovoltaic Modules" J. of Solar Energy Engg., Transcations of the ASME, Vol.136,MAY2014.
[11] Vidya Ganapati et al., Infrared birefringence imaging of residual stress and bulk defects in multicrystalline silicon, Journal of Applied Physics 108, 063528 (2010)

[12] Fang Li, Study of Stress Measurement Using Polariscope, PhD Thesis, Georgia Institute of Technology, 2010
[13] G. Sarau et al., Residual Stress Measurements In Multicrystalline Silicon Bulk And Thin Film Solar Cells Using Micro-Raman Spectroscopy, 23rd European Photovoltaic Solar Energy Conference, 2008, Valencia, Spain.
[14] A.S. Budiman et al., "Enabling thin silicon technologies for next generation c- Si solar PV renewable energy systems using synchrotron X-ray microdiffraction as stress and crack mechanism probe" Solar Energy Materials & Solar Cells, 2014, Vol. 130, pp. 303-308.
[15] A.S. Budiman, "Enabling Thin Silicon Technology", Science Highlights, June 2013, Lawrwnce Berkeley National Laboratory (www-als.lbl.gov/index.php/science-highlights/industry-als/829-improving- thin-silicon-solar-cell-technology.html).
[16] Brent Fultz · James Howe, Transmission Electron Microscopy and Diffractometry of Materials, 3rd Ed., Springer, 2007
[17] Tamura N. et al., A Superbend X-Ray Microdiffraction Beamline at the Advanced Light Source, eScholorship, University of California Berkeley, USA, 2009
[18] A.S. Budiman, Probing Crystal Plasticity at the Nanoscales, Springer, 2015
[19] Gene E. Ice*, Judy W.L. Pang, Tutorial on x-ray microLaue diffraction, MATERIALS CHARACTERIZATION 60 (2009) 1191–1201
[20] Tamura N., XMAS: A Versatile Tool for Analyzing Synchrotron X-ray Microdiffraction Data, Chapter-4 of Strain and Dislocation Gradients from Diffraction, World Scientific, 2014.
[21] K. Chen, N. Tamura, W. Tang, M. Kunz, Y.C. Chou, K.N. Tu, Y.S. Lai, High precision thermal stress study on flip chips by synchrotron polychromatic X- ray microdiffraction, J. Appl. Phys. 107 (2010) 063502.
[22] M. A. Brown et al., A Comparison of X-Ray Microdiffraction and Coherent Gradient Sensing in Measuring Discontinuous Curvatures in Thin Film: Substrate Systems, J. of Applied Mech., Transcations of the ASME, Vol.73, pp. 723-729, Sep2006.